Mansoura Engineering Journal

Volume 48 | Issue 5 Article 4

August 2023

Low loss hybrid plasmonic waveguide with graphene multilayers

Hala Mossad I. Hassan
Department of Electronics and Communications Engineering, Faculty of Engineering, University of Mansoura, Mansoura 35516, Egypt

Nihal F. F. Areed
Department of Electronics and Communications Engineering, Faculty of Engineering, University of Mansoura, Mansoura 35516, Egypt

H. A. EL-Mikati
Department of Electronics and Communications Engineering, Faculty of Engineering, University of Mansoura, Mansoura 35516, Egypt

Mohamed Farhat O. Hameed
Centre for Photonics and Smart Materials, Zewail City of Science, Technology and Innovation, October Gardens, 6th of October City, Giza, 12578

S. S. A. Obayya
Department of Electronics and Communications Engineering, Faculty of Engineering, University of Mansoura, Mansoura 35516, Egypt, sobayya@zewailcity.edu.eg

Recommended Citation

Hassan, Hala Mossad I.; Areed, Nihal F. F.; EL-Mikati, H. A.; Hameed, Mohamed Farhat O.; and Obayya, S. S. A. (2023) "Low loss hybrid plasmonic waveguide with graphene multilayers," *Mansoura Engineering Journal*: Vol. 48 : Iss. 5 , Article 4.
Available at: https://doi.org/10.58491/2735-4202.3067

ORIGINAL STUDY

Low-loss Hybrid Plasmonic Waveguide with Graphene Multilayers

Hala M.I. Hassan [a], Nihal F.F. Areed [a,b], Hamdi A. EL-Mikati [a], Mohamed F.O. Hameed [b,c,d], Salah S.A. Obayya [a,b,*]

[a] Department of Electronics and Communications Engineering, Faculty of Engineering, University of Mansoura, Mansoura, 35516, Egypt
[b] Centre for Photonics and Smart Materials, Zewail City of Science, Technology and Innovation, October Gardens, 6th of October City, Giza, 12578, Egypt
[c] Nanotechnology and Nanoelectronics Engineering Program, Zewail City of Science, Technology and Innovation, October Gardens, 6th of October City, Giza, 12578, Egypt
[d] Mathematics and Engineering Physics Department, Faculty of Engineering, University of Mansoura, Mansoura, 35516, Egypt

Abstract

A proposed design of a graphene-based hybrid plasmonic waveguide is presented to improve the propagation length with good confinement. The suggested design has multilayers of SiO_2-graphene/SiO_2 − GaAs − graphene/SiO_2. The full vectorial finite element method (FVFEM) is used to study the effective index (n_{eff}), propagation length (L_p), and normalized effective mode area (A_{eff}) of the supported hybrid plasmonic modes. In this investigation, the structure and the geometrical parameters are studied to achieve an ultra-small effective mode area with low propagation loss. The numerical results show that a long propagation length of 138 μm at a frequency of 3 THz is achieved with a normalized mode area of ~$10^{-5}\lambda^2$ and propagation loss of 0.0315 dB/μm. Therefore, the reported waveguide has advantages in terms of low propagation loss with good field confinement, which can be effectively used in integrated photonic devices.

Keywords: Graphene, Plasmonic, Sub-wavelength confinement, THz waveguide

1. Introduction

Surface plasmons (SPs), combined with free electrons and electromagnetic field oscillation at the metal/dielectric interface, can confine the light in a very small area beyond the diffraction limit. Therefore, SPs have sparked a lot of research in different applications including waveguiding (Teng et al., 2020a; Mabrouki and Latrach, 2015), sensing (Azzam et al., 2016), optical antennas (Obayya et al., 2015), data storage (El-Rabiaey et al., 2016; Areed and Obayya, 2014), optical filters (Almewafy et al., 2019), and solar cells (Hussein et al., 2014; Areed et al., 2018). The SPs in the visible to near-infrared frequency range are typically supported by noble metals such as gold and silver. As a result, a variety of plasmonic waveguide structures have been examined and proposed such as the long-range plasmonic waveguide (Oulton et al., 2008), dielectric-loaded plasmon waveguide (Weeber et al., 2017), metallic nanowire waveguide (Bian et al., 2018), metallic slot waveguide (Zheng et al., 2018), and hybrid plasmonic waveguide (Chen et al., 2012). Sub-wavelength confinement has been reported using surface plasmon polariton modes in different plasmonic waveguides (Oulton et al., 2008). In this context, dielectric-loaded plasmonic waveguides have been introduced using polymer ridges with CMOS-compatible metallic thin films (Weeber et al., 2017). Further, a silicon nano-rib loaded with a metallic nanowire at 1.55 μm was designed (Bian et al., 2018) with a propagation length of 2.2−60.2 μm and a mode area of ($\lambda^2/4.5 \times 10^5 \lambda^2/7 \times 10^3$). Hybrid plasmonic slot-rib waveguide has been presented at a wavelength of 1.55 μm (Zheng et al., 2018) with mode effective area in the range of λ^2/1000000-λ^2/100000) along with a reasonable propagation length (5 μm−25 μm). A thin metallic film has been placed

Received 30 March 2023; revised 12 June 2023; accepted 13 June 2023.
Available online 18 August 2023

* Corresponding author at: Zewail City of Science and Technology, Egypt.
E-mail address: sobayya@zewailcity.edu.eg (S.S.A. Obayya).

https://doi.org/10.58491/2735-4202.3067

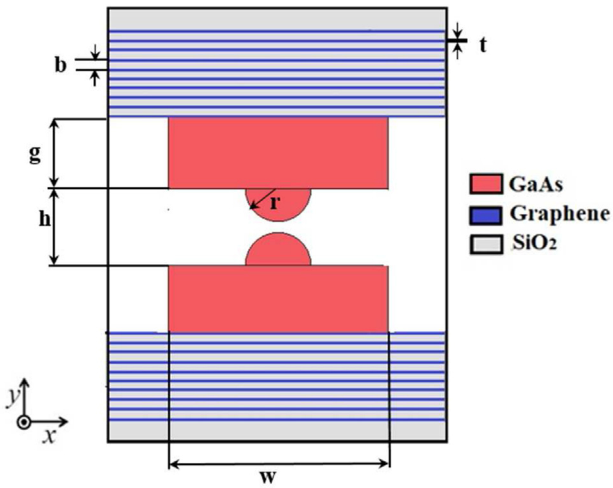

Fig. 1. The reported hybrid graphene plasmonic waveguide in the x-y plane.

between two identical dielectric nanowires (Chen et al., 2012) with a propagation length of 434 μm and a mode area of 0.0096 μm^2 at 1.55 μm. However, there is a tradeoff between low modal loss and device miniaturization with modal field containment. In the terahertz (THz) range, the plasmonic waves are extremely low at the metal surface, limiting their use at the nanoscale.

Graphene has unique photonics, electronics, and plasmonic features with a single layer of a combined atomic carbon sheet (Grigorenko et al., 2012). Furthermore, SP polariton (SPP) transmission can be stimulated and promoted by graphene layers in the THz to mid-infrared (mid-IR) spectrum, which typically ranges from 10 to 4000 cm^{-1} (Polini, 2016). Also, graphene-based plasmons have advantages compared with conventional plasmonic materials in terms of sub-wavelength mode containment and strong light−matter interactions. Further, a gate voltage can actively adjust the chemical potential for graphene to improve the wave guidance performance. Several graphene plasmonic waveguides for guiding SPP with deep sub-wavelength were proposed using graphene films (Robinson et al., 2010), graphene nanoribbons (Tran et al., 2017), graphene wedge/groove (Liu et al., 2013), graphene-coated nano-spheres (Christensen et al., 2015), and graphene-coated nanowires (Teng et al., 2020b). Dielectric-loaded

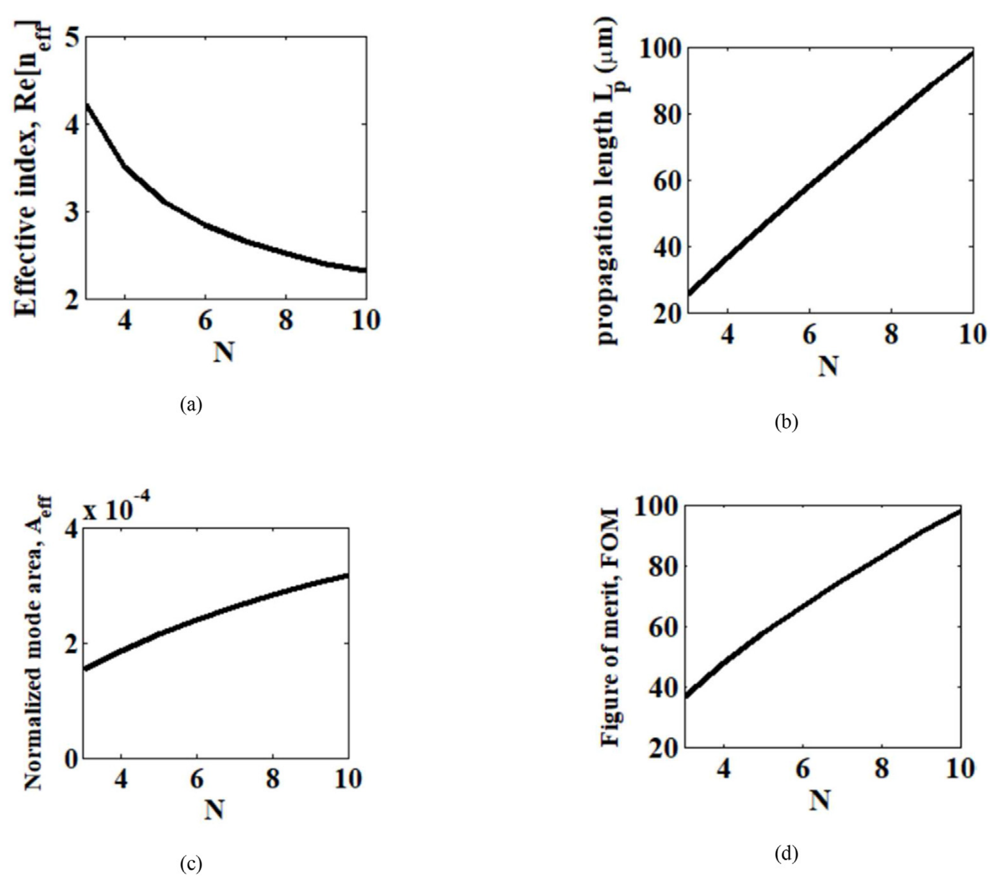

Fig. 2. Variation of (a) the real effective index n_{eff}, (b) L_p, (c) normalized A_{eff}, and (d) FOM of the fundamental hybrid mode with the number of graphene layers N, while the other geometrical parameters are fixed at g = 5 μm, h = 1 μm, r = 0.5 μm, w = 20 μm, and b = 14 nm.

graphene plasmonic waveguide has been also introduced based on a dielectric strip with a graphene sheet (Xu et al., 2015). Terahertz dielectric-loaded graphene waveguide has been studied where the cutoff wavelength of higher order modes has been calculated (Teng and Wang, 2021). In the study by Zhou et al., 2014, high-density polyethylene (HDPE) and GaAs have been used as high-index and low-index dielectric layers in graphene-based hybrid plasmonic waveguides. Small mode area and propagation length of 232.6 μm^2 and 127 μm, respectively, have been obtained at 3 THz. In the study by Rezaei et al., 2015, a strip-assisted hybrid plasmonic waveguide has been suggested with a propagation length of 820 μm, power confinement ratio of 0.65, and normalized mode area (A_{eff}) of 0.03 at 3 THz. Further, a two-layered MgF_2–Si structure covered by a graphene-coated nano-wire is reported in Ref (Hajati and Hajati, 2016) with a long propagation length of 13.91 μm. In addition, a long-range SPP hybrid waveguide has been proposed using a graphene material with a long propagation length of 10 μm at 30 THz and normalized A_{eff} of 10^{-7} (Liu et al., 2016). A distributed Bragg reflector-based hybrid plasmonic terahertz waveguide is proposed at 3 THz in the study by Mahankali et al., 2022. The normalized mode area was 3.733×10^{-3} μm^2 with a propagation length of 16.8 μm. Multilayer graphene-based hybrid plasmonic waveguide has been introduced using the cylindrical dielectric waveguide and hyperbolic metamaterials with a few millimeters of propagation length with a mode area of 10^{-3} μm^2 at a wavelength of 100 μm (Huang and Huang, 2021). Further, a compact ultralow-loss graphene-based multilayer hybrid plasmonic waveguide has been suggested with a propagation length of 45.28 mm and a mode area of 0.0547 μm^2 at $\lambda = 1550$ nm (Bahrami-Chenaghlou et al., 2023). However, the graphene plasmon is affected by high absorption loss in the mid-infrared waveband, as graphene contains the majority of the light energy. In addition, graphene plasmonic wave propagation is still relatively small. The main challenge for the graphene-based SPP waveguide is therefore to dramatically improve the propagation length while retaining the existing degree of containment. Graphene-based hybrid plasmonic waveguides (GHPW) have the advantages of graphene and traditional hybrid plasmonic waveguides. They combine deep sub-wavelength and high-performance characteristics.

In this study, a modified hybrid plasmonic terahertz waveguide is reported and optimized with an ultra-small mode area (~$10^{-5}\lambda^2$), which is smaller than those of the traditional graphene plasmonic waveguides (Zhou et al., 2014; He et al., 2018). This is achieved by improving the coupling between the fundamental dielectric waveguide mode and the surface plasmon polaritons mode (Iorsh et al., 2013). The suggested structure consists of an

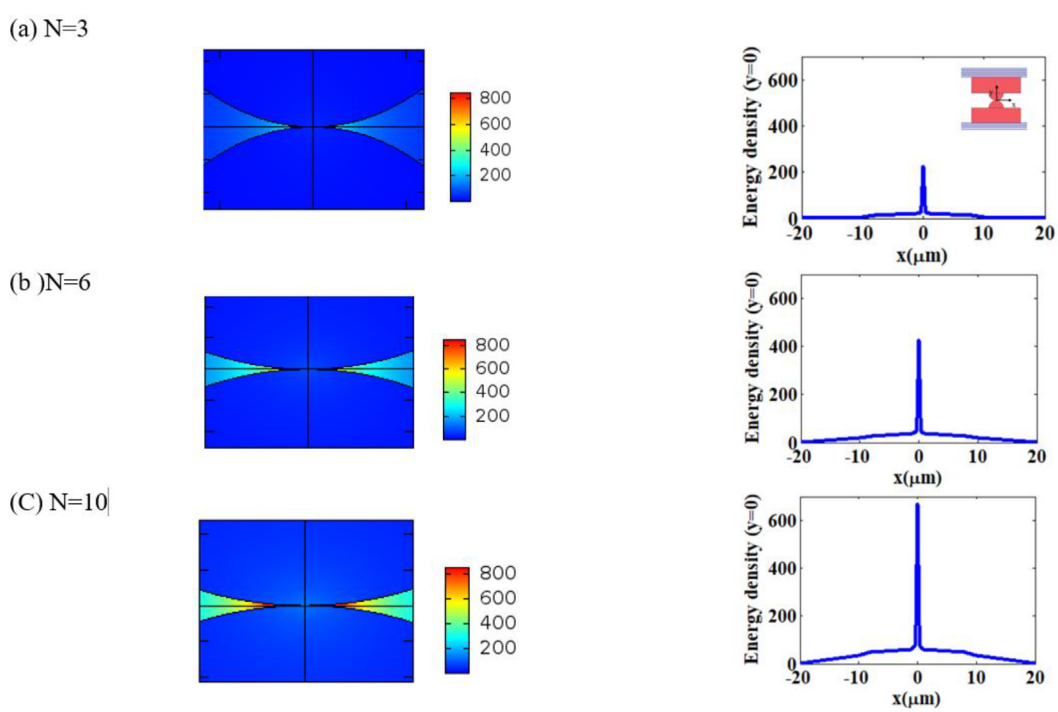

Fig. 3. The 2D and 1D (at y = 0) energy density distributions of the fundamental hybrid mode using N= (a) 3 layers, (b) 6 layers, and (c) 10 layers at g = 5 μm, h = 1 μm, r = 0.5 μm, w = 20 μm, and b = 14 nm.

SiO_2–graphene/SiO_2–GaAs–graphene/SiO_2 multilayer. The reported structure has the advantage of using multilayers of graphene (Liu et al., 2018; Qin et al., 2014) to improve the propagation properties. The impact of the structural geometrical parameters on the modal characteristics of the reported waveguide is carried out using full vectorial finite-element methods (Obayya et al., 2000). In this context, the effective index (n_{eff}), propagation length (L_p), and normalized mode area (A_{eff}) are studied thoroughly. A small mode area of $10^{-5}\lambda^2$ is achieved with a propagation loss of 0.0315 dB/μm at f = 3 THz, which is smaller than those reported in Refs (He et al., 2018, 2019a, 2019b, 2021). The reported waveguide has a good potential for highly efficient light transmission in integrated photonic circuits.

2. Design considerations and numerical results

Fig. 1 shows the schematic diagram of the SiO_2–graphene/SiO_2–GaAs–graphene/SiO_2- multilayer structure. Two identical outer silica layers and two identical inner graphene multilayers are symmetrically placed on both sides of the GaAs layer. The GaAs layer consists of two rectangular waveguides with thickness g and width w. The separation between the rectangular waveguides is labeled as h. Further, a micro semicircular rib with radius r is used, with a high-index material of GaAs (n = 3.5). In addition, 10 graphene layers are used with a thickness of t, which are separated by silicon layers with a thickness of b. The FVFEM (Obayya et al., 2000) is used via COMSOL Multiphysics software [https://www. comsol. com] to analyze the waveguide characteristics. The graphene permittivity can be determined by applying (Hanson, 2008) the following equation:

$$\varepsilon_g = 1 + i\frac{\sigma_g}{\varepsilon_0 \omega t} \tag{1}$$

where t = 0.5 nm is the monolayer graphene thickness; ε_0 is the permittivity of free space; and ω is the angular frequency. According to Kubo's formulation (Ziegler, 2007), the interband and

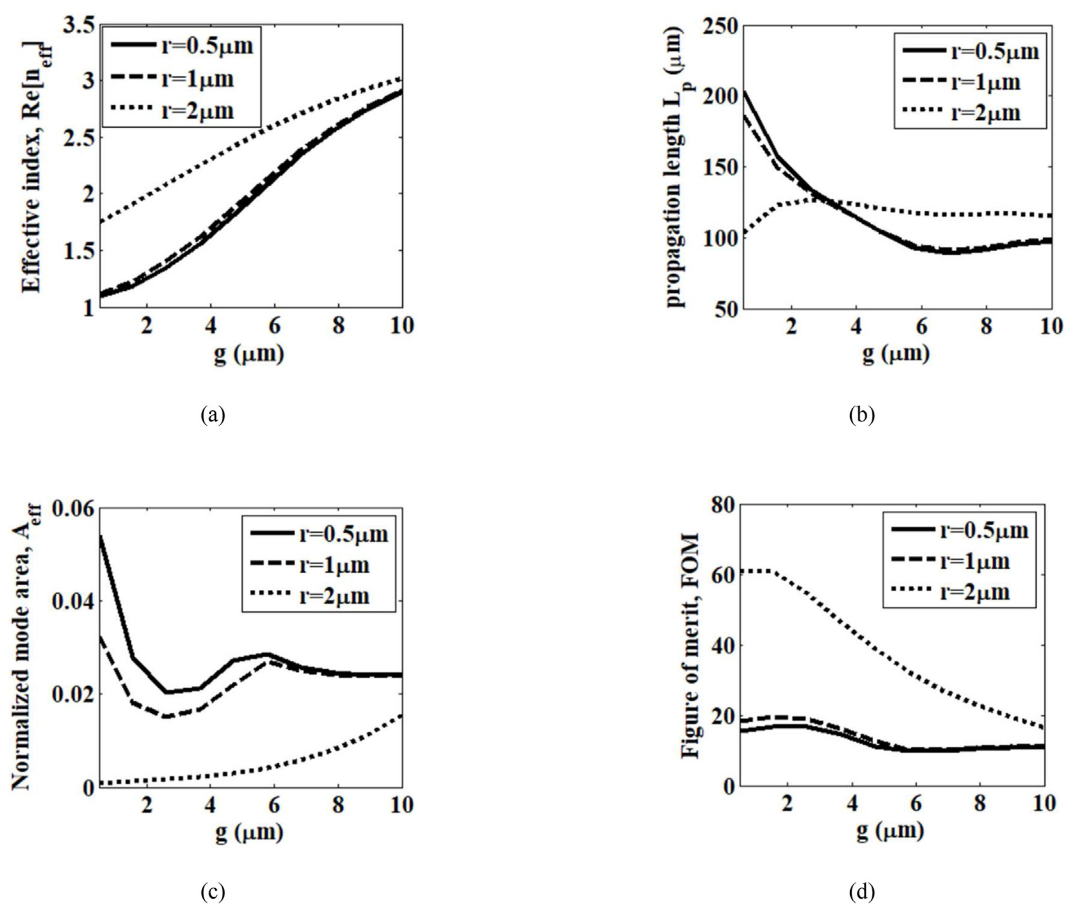

Fig. 4. The dependence of the (a) effective index n_{eff}, (b) L_p, (c) normalized A_{eff}, and (d) FOM of the fundamental hybrid mode on the diameter of the GaAs d, while $w = 25\ \mu m$, $b = 14\ nm$, $h = 4\ \mu m$, and $\mu_c = 0.5\ eV$.

intraband contributions to the graphene surface conductivity are as follows:

$$\sigma_g = \sigma_{intra} + \sigma_{inter} \tag{2}$$

$$\sigma_{intra} = \frac{2je^2 k_B T}{\pi \hbar^2 (\omega + j/\tau)} \ln\left(2\cosh\left(\frac{\mu_c}{2k_B T}\right)\right) \tag{3}$$

$$\sigma_{inter} = \frac{e^2}{4\hbar}\left[\frac{1}{2} + \frac{1}{\pi}\arctan\left(\frac{\hbar\omega - \mu_c}{2k_B T}\right) - \frac{j}{2\pi}\ln\frac{(\hbar\omega + 2\mu_c)^2}{(\hbar\omega - 2\mu_c)^2 + (2k_B T)^2}\right] \tag{4}$$

where T is the temperature; k_B is Boltzmann's constant; ħ is the reduced plank constant; μ_c is graphene's chemical potential; τ is the time of electron relaxation; and e is the electron's charge. Here, T = 300 K, τ = 0.5 ps, and μ_c = 0.5 eV.

In this study, the n_{eff}, the normalized A_{eff}, L_p, and figure of merit (FoM) (Chowdhury, 2011) of the supported hybrid modes are studied and analyzed. The FoM is calculated using the equation

$$FOM = \frac{Lp}{2 * \sqrt{\frac{A_{eff}}{\pi}}} \tag{5}$$

The propagation length is given by

$$L_{prop} = \frac{\lambda}{4\pi Im(n_{eff})} \tag{6}$$

The effective mode area A_m can be found by the formula (Chowdhury, 2011)

$$A_m = \frac{\iint (W(r) dA}{\max(W(r))} \tag{7}$$

The W(r) is the energy density of the supported mode with electric field E(r) and magnetic field H(r), which is defined by the equation

$$W(r) = \frac{1}{2}\mu_0 |H(r)|^2 + \frac{1}{2} Re\left\{\frac{d[w\varepsilon(r)]}{dw}\right\}|E(r)|^2 \tag{8}$$

where μ_0 is the free space magnetic permeability, and ε(r) is the dielectric permittivity. It is required to improve the field confinement of the supported modes with long propagation lengths and minimum propagation losses.

3. Numerical results of plasmonic

To achieve long propagation length with strong field confinement, the geometrical parameters of the reported structure are studied. First, the effect of the number of graphene layers is investigated. Fig. 2 shows the mode properties' dependence on the

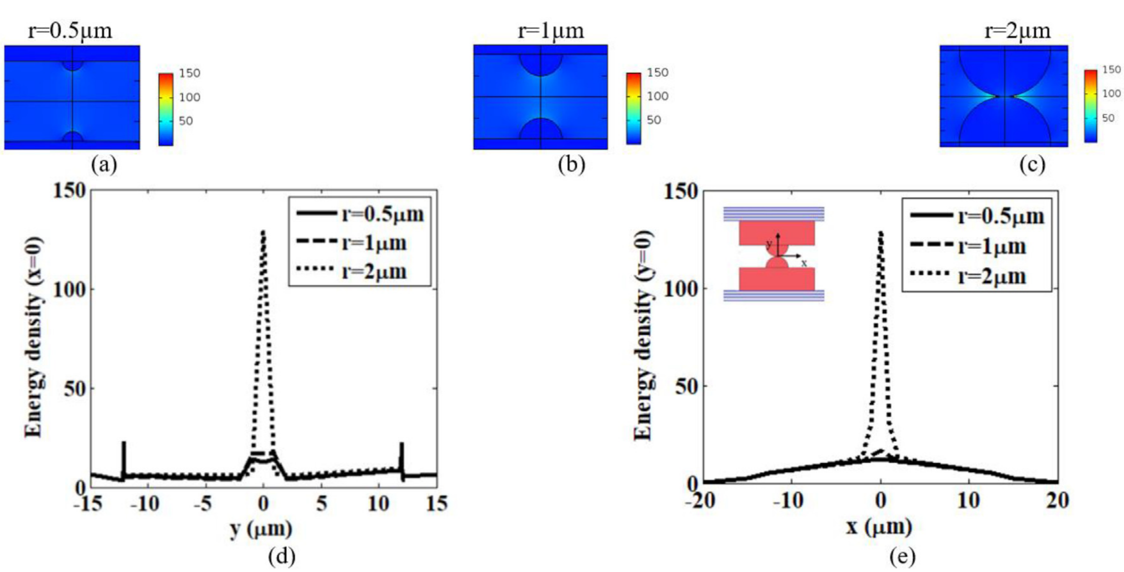

Fig. 5. (a–c) 2D energy densities of the supported fundamental hybrid mode, while d and e shows the 1D energy density distributions along the vertical and horizontal axes. The suggested structure's cross-section is shown in the insert of e at w = 25 μm, b = 14 nm, g = 10 μm, h = 4 μm, and μ_c = 0.5 eV.

numbers of graphene layers N. Here, N varies from 3 to 10 layers. However, the other geometrical parameters are fixed at $g = 5$ μm, $h = 1$ μm, $r = 0.5$ μm, $w = 20$ μm, and $b = 14$ nm. Fig. 2a shows that the effective index n_{eff} increases and then decreases by increasing the number of graphene layers N. As N increases, the propagation length L_p and figure of merit FOM increase as shown in Fig. 2b, d. It is also evident that the normalized mode area A_{eff} increases slightly from 1.5×10^{-4} to 3.17×10^{-4} as shown in Fig. 2c. It can be noticed that the propagation length L_p increases from 25.4 μm to 98.2 μm, and the FoM increases from 36 to 97 by increasing N from 3 layers to 10 layers. Therefore, N = 10 is taken with high propagation length and sub-wavelength mode confinement. The effective conductivity of the fundamental volume plasmon polariton modes with a significant electric field is approximately Nσ, and the mode field profile widens moderately as N increases, according to the analytical formula (Smirnova et al., 2014) of a multilayer graphene waveguide. Hence, when N grows, larger L_p and A_{eff} are due to the strong coupling between the volume plasmon polariton and major electric fields. Fig. 3 shows the 2D energy density of the supported modes at N = 3, 6, and 10 layers, while the 1D plots are shown on the right at y = 0. The optical energy is confined around a micro semicircular rib as N increases. Therefore, the A_{eff} is increased [Fig. 2c] with a significant reduction of ohmic losses. When N increases, the enhancement of the field peak, as shown in Fig. 3, compensates for the full width at half maximum along y = 0. Further, the number of graphene layers can improve the achieved optical energy.

Next, the effect of radius r is studied. Fig. 4 shows the variation of the n_{eff}, L_p, A_{eff}, and FoM, depending on thickness g at various micro semicircular rib r values (0.5 μm, 1 μm, and 2 μm) within the g range of 0.5–10 μm. It can be seen that n_{eff} increases, while the L_p and FoM decrease as the distance g increases. Therefore, at increased micro semicircular rib r, smaller A_{eff}, L_p high, and high FOM can be obtained with strong optical confinement as shown in Fig. 4b–d.

Especially when $r = 2$ μm, a minimum of A_{eff} of [~9×10^{-4} ($\lambda^2/4$)] is achieved at $g = 0.5$ μm with L_p of 103.5 μm and FOM of 61 as illustrated in Fig. 4a–c. It can be noticed that to obtain better performance using the micro semicircular rib, r equals $h/2$. Fig. 5 shows the 2D energy density distribution of the supported hybrid mode at different micro semicircular rib radii (r). It may be seen that at $r = 0.5$

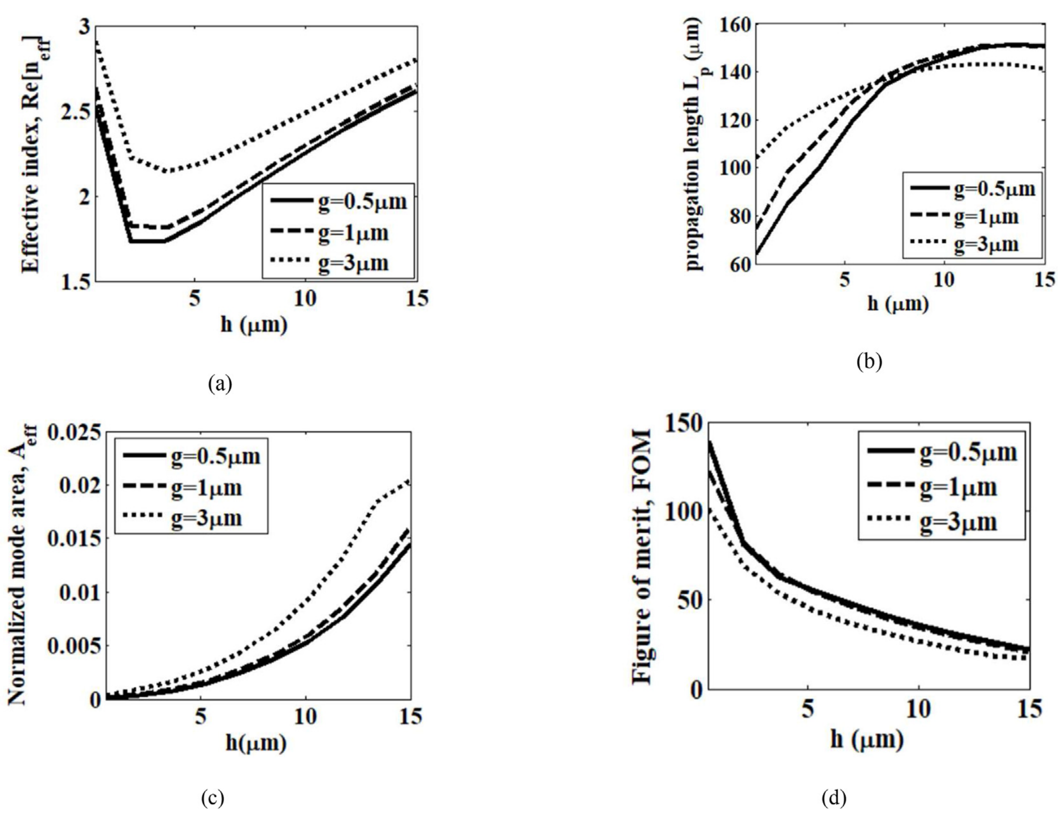

Fig. 6. Variation of the (a) n_{eff}, (b) L_p, (c) normalized A_{eff}, and (d) FOM of the fundamental hybrid mode with the diameter of the GaAs d, while $w = 25$ μm, $b = 14$ nm, $r = h/2$, and $\mu_c = 0.5$ eV.

μmas shown in Fig. 5a; low-energy flow density distribution exists in graphene multilayers due to the weak coupling between plasmonic and optical modes. It may be seen that when the distance r increases, the optical energy increases owing to the strong coupling with the SPP mode. Due to the increase in the area of a high-index region, the mode field is more concentrated toward the region between two micro semicircular ribs (Fig. 5d and e) showing 1D energy density distributions along the vertical (at y = 0) and horizontal (at x = 0) directions as *r* changes from 0.5 μm to 2 μm. It is evident from Fig. 5e that the energy density in the gap area is sharply increased as the distance *r* increases to 2 μm. Therefore, the optical energy of the supported mode can be confined in the gap, when a large *r* is used.

The impact of the rectangular waveguide is next investigated. Fig. 6 illustrates the variation of the real part of the effective index n_{eff}, L_p, normalized A_{eff}, and FoM, with the distance *h* at various thicknesses and *g* values (0.5 μm, 1 μm, and 3 μm) within the range 0.5−15 μm. It can be seen that n_{eff}, L_p, *and* A_{eff} increase, while the FoM decreases as the distance *g* increases. Therefore, at a reduced distance *h*, a smaller A_{eff} and high L_p can be obtained with strong optical confinement as shown in Fig. 6b−d. At $g = 0.5$ μm, A_{eff} of [6.6 × 10^{-5} ~14.4 × 10^{-3} ($\lambda^2/4$)] can be achieved, where an L_p of (64 μm,~150 μm) and an FOM of (139~22) are achieved as illustrated in Fig. 6a−d. These results show that the distance *g* and h can be simultaneously controlled to achieve deep sub-wavelength confinement with the improved overall optical performance. The numerical simulations indicate that by designing the proposed geometric structure, a smaller A_{eff} [~6.6 × 10^{-5} ($\lambda^2/4$)] can be achieved at a propagation length of 64 μm. Fig. 7 illustrates the energy density of the 2D and 1D (at y = 0) electric field distributions of the supported modes at different distances *h:* 1 μm, 7 μm, and 15 μm. The optical energy of the supported mode is improved by decreasing the distance *h*.

To achieve high efficiency with tunable performance, the effect of the applied potential on the graphene layer is studied. Fig. 8 shows the effect of the chemical potential of the graphene μ_c on the n_{eff}, A_{eff}, *and* L_p of the fundamental hybrid mode at $w = 25$ μm and b = 14 nm. It can be seen that the effective index n_{eff} decreases monotonically, while L_p

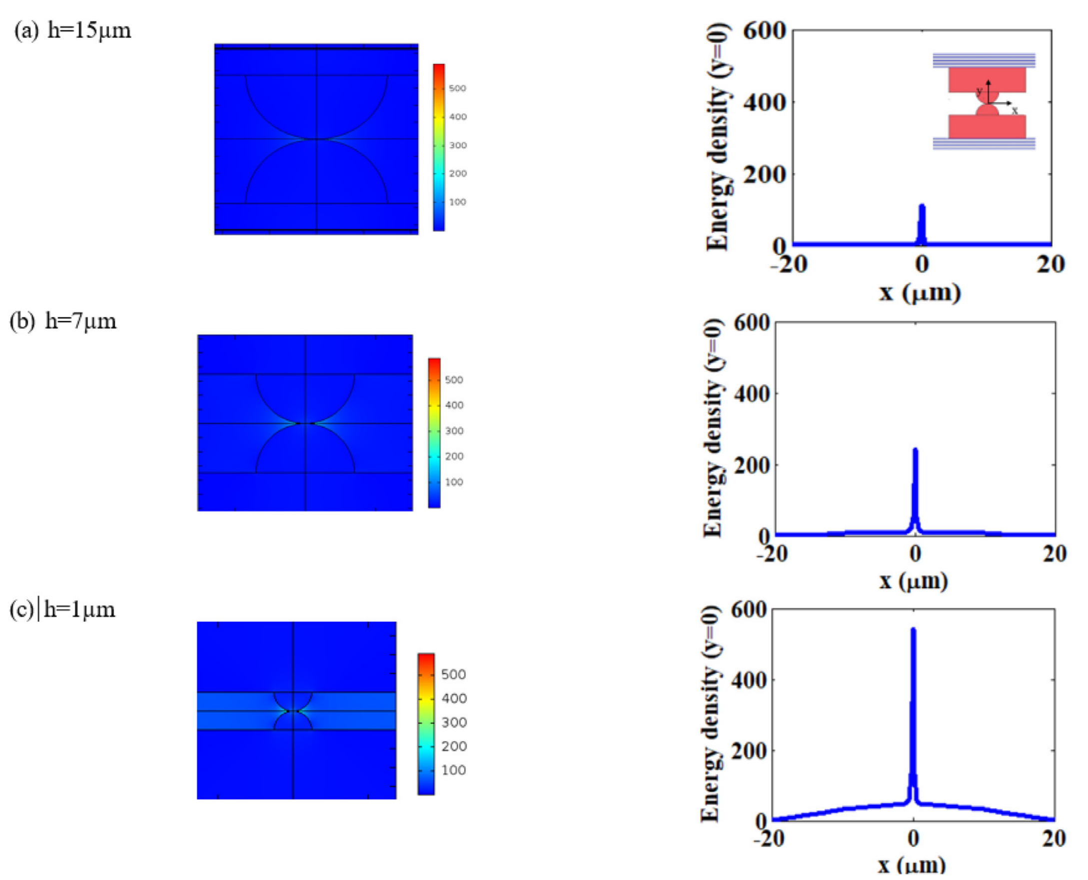

Fig. 7. 2D and 1D (at y = 0) plots of the energy density distributions of the supported fundamental hybrid mode at different h values of 15 μm, 7 μm, and 1 μm at g = 3 μm, w = 25 μm, b = 14 nm, r = h/2, and μ_c = 0.5 eV.

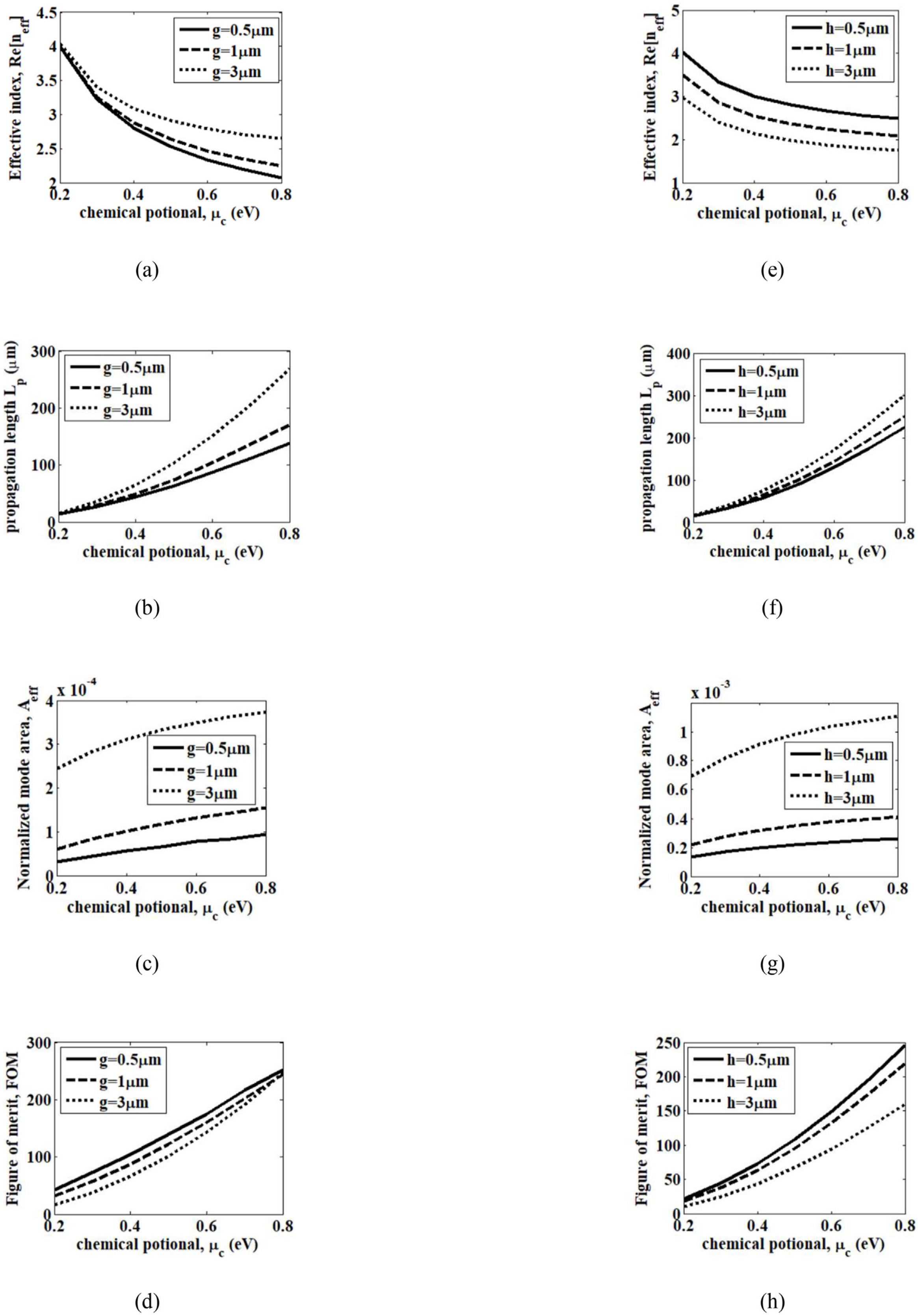

Fig. 8. Variation of (a) n_{eff}, (b) L_p, and (c) normalized A_{eff}, and (d) FoM with the chemical potential of graphene μ_c at $h = 0.5$ μm and different g values. The dependence on the chemical potential μ_c at $g = 2$ μm and different values of h are shown in (e, f, g, and h). The other parameters are taken as $w = 25$ μm, $r = h/2$, and $b = 14$ nm.

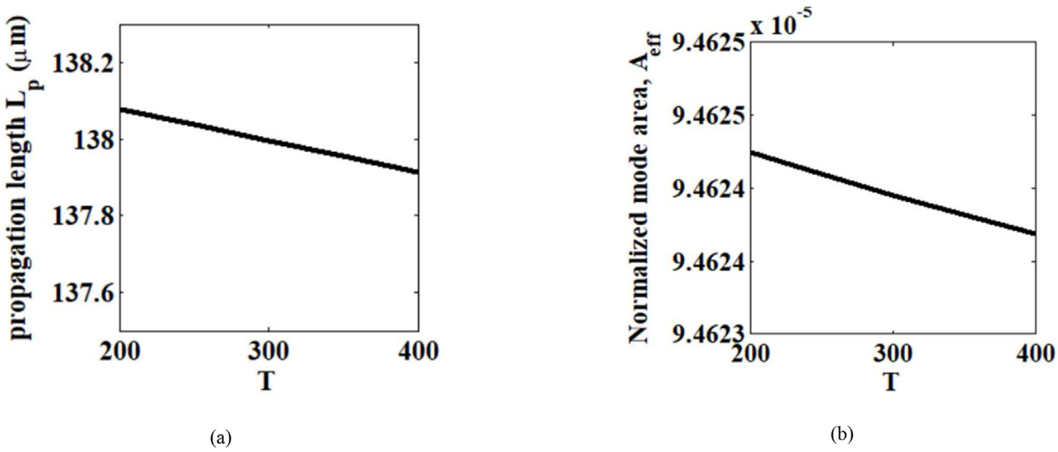

Fig. 9. Variation of (a) L_p and (b) normalized A_{eff} of the supported hybrid mode with temperature T, while the other geometrical parameters are fixed at g = 0.5 μm, h = 0.5 μm, w = 25 μm, and b = 14 nm.

and FOM increase monotonically with the increase of μ_c. In this circumstance, A_{eff} of [3×10^{-5}~9.5×10^{-5}] can be achieved where the chemical potential μ_c can be tuned to achieve relative lengths of propagation (13.6 μm–138 μm). When μ_c is increased, the conductivity value of graphene (σ_g) will be increased, while the imaginary part of the effective index (Im (n_{eff}) will be reduced. Then, the graphene loss is low at large μ_c values. The proposed structure has deep sub-wavelength confinement, which is very promising for the integration of compact photonic devices.

The effect of the temperature on the graphene layer used in the proposed design with its optimal geometries (g = 0.5 μm, h = 0.5 μm, w = 25 μm, b = 14 nm) is next studied. Fig. 9 shows the impact of temperature on the L_p and A_{eff} of the fundamental hybrid mode. It can be observed that the temperature has a negligible effect on the normalized A_{eff} as well as the propagation length over the temperature ranging from 200 K to 400.

The optical properties of the reported waveguide are compared with those presented in the literature as shown in Table 1. It is revealed from this table that the reported waveguide has a much lower loss than the previously graphene plasmonic waveguides (He et al., 2018, 2019a, 2019b, 2021). Thereby, a mode area of about (~$10^{-5}\lambda^2$) with a long propagation length of 138 μm can be achieved. This is a significant improvement over the previous structures (Zhou et al., 2014; He et al., 2018, 2019a, 2019b, 2021). Furthermore, the reported waveguide has stronger optical confinement and longer propagation length than the proposed waveguide with GaAs and graphene (He et al., 2018, 2019a, 2019b, 2021). It is evident from Table 1 that the suggested design has a propagation length 3 times longer than that previously designed in the study by He et al., 2018 with the same material. Compared with the recently published designs presented by Huang and Huang (2021) and Bahrami-Chenaghlou et al. (2023), which are operating at λ = 100 μm and 1550 nm, respectively, the suggested hybrid plasmonic terahertz waveguide based on multilayers of graphene has a propagation length of 138 μm with a mode normalized area of ~$10^{-5}\lambda^2$ at f = 3 THz (λ = 100 μm). This improvement is due to using multilayers of graphene that can be used to realize compact hybrid waveguides.

Table 1. Optical properties of the reported waveguide compared with those suggested in the literature in terms of L_p, normalized A_{eff}, and FoM.

Design	Wavelength (μm)	Material	L_{prop} (μm)	Normalized A_{eff}	FoM
He et al., 2019a	100	Graphene, GaAs, HDPE	~25.1/21.3	~2.6×10^{-4}/1.5×10^{-4}	~54.6/60.1
He et al., 2019b	100	Graphene, GaAs, SiO_2	~ 35.4	~$10^{-4}\lambda^2$	N/A
Zhou et al., 2014	100	Graphene, GaAs, HDPE	~127	~10^{-2}	N/A
He et al., 2018	100	Graphene, GaAs, SiO_2	~15/26	~0.0032 (λ^2/4)/0.0018 (λ^2/4)	N/A
He et al., 2021	100	Graphene, GaAs, HDPE	tens of micrometers	~$10^{-4}\lambda^2$	N/A
Huang and Huang, 2021	100	Graphene, Si, SiO_2	few millimeters	~10^{-3}	N/A
Bahrami-Chenaghlou et al., 2023	1.55	Graphene	45.28 mm	0.0547	N/A
Proposed design	100	Graphene, GaAs, SiO_2	~13/138	~3.1×10^{-5}/9.46×10^{-5}	~43.2/251.6

4. Conclusion

A hybrid plasmonic multilayer-graphene waveguide is proposed and investigated for deep terahertz sub-wavelength confinement. The modal analysis of the reported waveguide is made using FVFEM. The numerical results show that the suggested normalized mode area could be very small ($\sim 10^{-5}\lambda^2$) with a long propagation length of 138 μm. The reported structure has also low propagation loss with good mode confinement. Therefore, the structure has a good potential capacity for developing THz waveguide with compact field confinement for photonic integrated circuits.

Authors' contribution

Nihal F. F. Areed, Mohamed Farhat O. Hameed, and Hala Mossad I. Hassan: conceived the presented idea. Hala Mossad I. Hassan developed the theory and performed the computations. Mohamed Farhat O. Hameed verified the analytical methods and supervised the findings of this work. Hala Mossad I. Hassan, Nihal F. F. Areed, Mohamed Farhat O. Hameed, Hamdi El Mikati, and S. S. A. Obayya discussed the results, reviewed them, and contributed to the final manuscript.

Conflicts of interest

The authors would like to clarify that there are no financial/non-financial interests that are directly or indirectly related to the work submitted for publication.

References

Almewafy, B.H., Areed, N.F., Hameed, M.F.O., Obayya, S.S., 2019. Modified D-shaped SPR PCF polarization filter at telecommunication wavelengths. Opt. Quant. Electron. 51, 1−14.

Areed, N.F., Obayya, S.S., 2014. Multiple image encryption system based on nematic liquid photonic crystal layers. J. Lightwave Technol. 32, 1344−1350.

Areed, N.F., El-Wasif, Z., Obayya, S., 2018. Nearly perfect metamaterial plasmonic absorbers for solar energy applications. Opt. Quant. Electron. 50, 1−12.

Azzam, S.I., Hameed, M.F.O., Shehata, R.E.A., Heikal, A., Obayya, S.S., 2016. Multichannel photonic crystal fiber surface plasmon resonance based sensor. Opt. Quant. Electron. 48, 142.

Bahrami-Chenaghlou, F., Habibzadeh-Sharif, A., Ahmadpour, A., 2023. Systematic design and analysis of a compact ultra-low loss graphene-based multilayer hybrid plasmonic waveguide. Photon. Nanostruct. Fundam. Appl. 53, 101088.

Bian, Y., Ren, Q., Kang, L., Yue, T., Werner, P.L., Werner, D.H., 2018. Deep-subwavelength light transmission in hybrid nanowire-loaded silicon nano-rib waveguides. Photon. Res. 6, 37−45.

Chen, L., Zhang, T., Li, X., Huang, W., 2012. Novel hybrid plasmonic waveguide consisting of two identical dielectric nanowires symmetrically placed on each side of a thin metal film. Opt. Express 20, 20535−20544.

Chowdhury, Y., 2011. Plasmonic Waveguides: Design and Comparative Study, ʻ ed.

Christensen, T., Jauho, A.-P., Wubs, M., Mortensen, N.A., 2015. Localized plasmons in graphene-coated nanospheres. Phys. Rev. B 91, 125414.

El-Rabiaey, M.A., Areed, N.F., Obayya, S.S., 2016. Novel plasmonic data storage based on nematic liquid crystal layers. J. Lightwave Technol. 34, 3726−3732.

Grigorenko, A.N., Polini, M., Novoselov, K., 2012. Graphene plasmonics. Nat. Photonics 6, 749−758.

Hajati, M., Hajati, Y., 2016. High-performance and low-loss plasmon waveguiding in graphene-coated nanowire with substrate. JOSA B 33, 2560−2565.

Hanson, G.W., 2008. Dyadic Green's functions and guided surface waves for a surface conductivity model of graphene. J. Appl. Phys. 103, 064302.

He, X., Ning, T., Lu, S., Zheng, J., Li, J., Li, R., et al., 2018. Ultralow loss graphene-based hybrid plasmonic waveguide with deep-subwavelength confinement. Opt. Exp. 26, 10109−10118.

He, X., Ning, T., Pei, L., Zheng, J., Li, J., Wen, X., 2019a. Tunable hybridization of graphene plasmons and dielectric modes for highly confined light transmit at terahertz wavelength. Opt. Exp. 27, 5961−5972.

He, X., Ning, T., Zheng, J., Li, J., Pei, L., Wu, B., 2019b. Deep-subwavelength light transmission in hybrid graphene-dielectric slot waveguide. J. Opt. 21, 095001.

He, X., Ning, T., Pei, L., Zheng, J., Li, J., Wang, J., 2021. Deep subwavelength graphene-dielectric hybrid plasmonic waveguide for compact photonic integration. Res. Phys. 21, 103834.

Huang, C.-C., Huang, C.-C., 2021. Terahertz hybrid plasmonic waveguides with ultra-long propagation lengths based on multilayer graphene-dielectric stacks. Opt. Exp. 29, 39521−39535.

Hussein, M., Areed, N.F., Hameed, M.F.O., Obayya, S., 2014. Hybrid core semiconductor nanowires for solar cell applications. Numer. Simul. Optoelectron. Dev. 2014, 89−90.

Iorsh, I.V., Mukhin, I.S., Shadrivov, I.V., Belov, P.A., Kivshar, Y.S., 2013. Hyperbolic metamaterials based on multilayer graphene structures. Phys. Rev. B 87, 075416.

Liu, P., Zhang, X., Ma, Z., Cai, W., Wang, L., Xu, J., 2013. Surface plasmon modes in graphene wedge and groove waveguides. Opt. Exp. 21, 32432−32440.

Liu, J.-P., Zhai, X., Wang, L.-L., Li, H.-J., Xie, F., Xia, S.-X., et al., 2016. Graphene-based long-range SPP hybrid waveguide with ultra-long propagation length in mid-infrared range. Opt. Exp. 24, 5376−5386.

Liu, J.-P., Wang, W.-L., Xie, F., Luo, X., Zhou, X., Lei, M., et al., 2018. Efficient directional coupling from multilayer-graphene-based long-range SPP waveguide to metal-based hybrid SPP waveguide in mid-infrared range. Opt. Exp. 26, 29509−29520.

Mabrouki, A., Latrach, M., 2015. Wireless energy transfer: on the efficiency of low power rectenna topologies, chapter 3. In: Mescia, L. (Ed.), Innovative Materials and Systems for Energy Harvesting Applications. IGI Global, pp. 63−91.

Mahankali, P., Rao, T.R., Susila, M., 2022. Investigations on mode analysis of distributed Bragg Reflector based hybrid plasmonic Terahertz Waveguide. J. Phys. Conf. Ser. 2335 (1), 012012.

Obayya, S., Rahman, B.A., El-Mikati, H., 2000. New full-vectorial numerically efficient propagation algorithm based on the finite element method. J. Lightwave Technol. 18, 409.

Obayya, S., Areed, N.F.F., Hameed, M.F.O., Abdelrazik, M.H., 2015. Optical nano-antennas for energy harvesting. In: Innovative Materials and Systems for Energy Harvesting Applications. IGI Global, pp. 26−62.

Oulton, R.F., Sorger, V.J., Genov, D., Pile, D., Zhang, X., 2008. A hybrid plasmonic waveguide for subwavelength confinement and long-range propagation. Nat. Photon. 2, 496−500.

Polini, M., 2016. Tuning terahertz lasers via graphene plasmons. Science 351, 229−231.
Qin, C., Wang, B., Huang, H., Long, H., Wang, K., Lu, P., 2014. Low-loss plasmonic supermodes in graphene multilayers. Opt. Exp. 22, 25324−25332.
Rezaei, M., Rasekh, P., Safian, R., 2015. A stripe-assisted hybrid plasmonic waveguide for the propagation of terahertz waves. IEEE Photon. Technol. Lett. 27, 2288−2291.
Robinson, J.T., Burgess, J.S., Junkermeier, C.E., Badescu, S.C., Reinecke, T.L., Perkins, F.K., et al., 2010. Properties of fluorinated graphene films. Nano Lett. 10, 3001−3005.
Smirnova, D., Iorsh, I., Shadrivov, I., Kivshar, Y.S., 2014. Multilayer graphene waveguides. JETP Lett. 99, 456−460.
Teng, D., Wang, K., 2021. Theoretical analysis of terahertz dielectric−loaded graphene waveguide. Nanomaterials 11, 210.
Teng, D., Wang, K., Huan, Q., Chen, W., Li, Z., 2020a. High-performance light transmission based on graphene plasmonic waveguides. J. Mater. Chem. C 8, 6832−6838.
Teng, D., Wang, K., Li, Z., 2020b. Graphene-coated nanowire waveguides and their applications. Nanomaterials 10, 229.
Tran, V.-T., Saint-Martin, J., Dollfus, P., Volz, S., 2017. Optimizing the thermoelectric performance of graphene nano-ribbons without degrading the electronic properties. Sci. Rep. 7, 1−11.
Weeber, J.-C., Arocas, J., Heintz, O., Markey, L., Viarbitskaya, S., Colas-des-Francs, G., et al., 2017. Characterization of CMOS metal based dielectric loaded surface plasmon waveguides at telecom wavelengths. Opt. Exp. 25, 394−408.
Xu, W., Zhu, Z., Liu, K., Zhang, J., Yuan, X., Lu, Q., et al., 2015. Dielectric loaded graphene plasmon waveguide. Opt. Exp. 23, 5147−5153.
Zheng, K., Song, J., Qu, J., 2018. Hybrid low-permittivity slot-rib plasmonic waveguide based on monolayer two dimensional transition metal dichalcogenide with ultra-high energy confinement. Opt. Exp. 26, 15819−15824.
Zhou, X., Zhang, T., Chen, L., Hong, W., Li, X., 2014. A graphene-based hybrid plasmonic waveguide with ultra-deep subwavelength confinement. J. Lightwave Technol. 32, 3597−3601.
Ziegler, K., 2007. Minimal conductivity of graphene: nonuniversal values from the Kubo formula. Phys. Rev. B 75, 233407.